Supplementary Material

Dual-Emission Luminescent Eu-MOF/g-C_3N_4 Nanomaterials: A Novel Bifunctional Platform for Aflatoxin B_1 Detection and Degradation

Wenjing Yin[a1], Ping Liu[a1], Wenzhen Du[b], Xuefang Lan[b,*], Qingli Yang[a,*], Yongchao Ma[b,*]

[a] *College of Food Science and Engineering, Qingdao Agricultural University, Qingdao, 266109, P. R. China*

[b] *College of Chemistry and Pharmaceutical Sciences, Qingdao Agricultural University, Qingdao, 266109, P. R. China*

***Corresponding authors:** yongchaoma@126.com.

[1] These authors contributed equally to this work.

1. Materials and instruments

1.1 Chemicals and reagents

Europium nitrate hexahydrate ($Eu(NO_3)_3·6H_2O$, 99.9%), 4,4',4'',4'''-(pyrazine-2,3,5,6-tetrayl) tetrabenzoic acid (H_4TCPP, 98%), melamine ($C_3H_6N_6$, 98%), N,N-dimethylformamide (DMF, AR, 99.5%), anhydrous ethanol (AR, 99.5%), methanol (for HPLC, ≥ 99.9%), and acetonitrile (for HPLC, ≥ 99.9%), aflatoxin B1 (AFB1, ≥ 98.0%), aflatoxin B2 (AFB2, ≥ 98.0%),sodium chloride (NaCl), potassium chloride (KCl), calcium chloride ($CaCl_2$), magnesium chloride hexahydrate ($MgCl_2·6H_2O$) and copper sulfate pentahydrate ($CuSO_4·5H_2O$), zinc chloride ($ZnCl_2$), cobaltous chloride hexahydrate ($CoCl_2·6H_2O$), aluminum chloride hexahydrate ($AlCl_3·6H_2O$), ferric chloride hexahydrate ($FeCl_3·6H_2O$), manganese chloride tetrahydrate ($MnCl_2·4H_2O$), ochratoxin A (OTA), zearalenone (ZEN), ascorbic acid (AA), gallic acid (GA), Lysine (Lys), Cysteine (Cys), maltose (ML), glucose (GL) were purchased from Macklin Biochemical Co., Ltd. (Shanghai, China). P-benzoquinone (PBQ, $C_6H_4O_2$), tert-Butano (BTA, $C_4H_{10}O$), Ethylene Diamine Tetraacetic Acid (EDTA, $C_{10}H_{16}N_2O_8$), were purchased from Sinopharm Chemical Reagent Co., Ltd. (Shanghai, China).

1.2 Instruments

The microscopic morphology of the synthesized materials was observed using a field emission scanning electron microscope (SEM, S-4800, Hitachi). The structures were analyzed by X-ray powder diffractometry (XRD, TD-3700, China) and Fourier transform infrared spectroscopy (FTIR, Nicolet iS10, USA). The light absorption characteristics were assessed using an ultraviolet-visible spectrometer equipped with an integrating sphere (UV–vis DRS, Shimadzu UV-3900, Japan). Photo-luminescence (PL) spectroscopy was conducted using a fluorescence spectrometer (PL, Shimadzu F7000, Japan). Time-resolved fluorescence spectroscopy (TRPL) was evaluated using the FLS1000 from Edinburgh Instruments, UK.

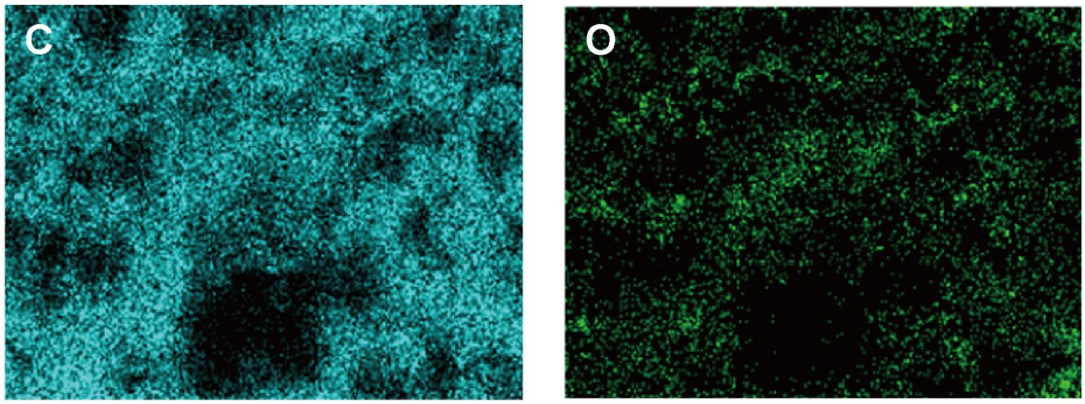

Fig. S1. C and N element mapping of Eu-MOF/g-C_3N_4.

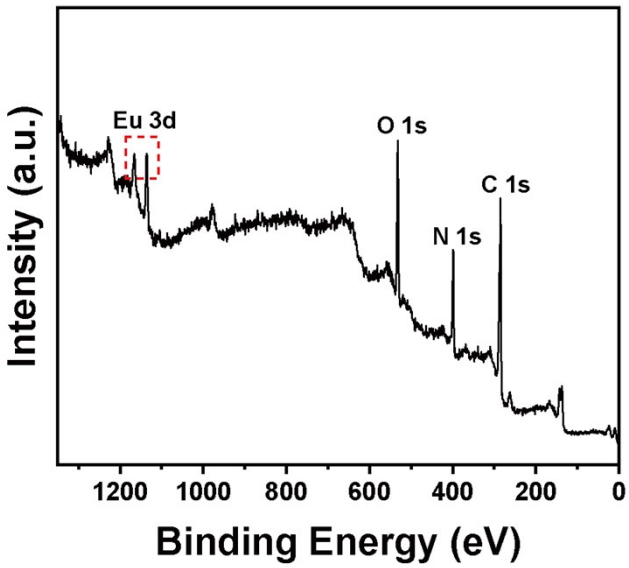

Fig. S2. XPS spectra of Eu-MOF/g-C_3N_4.

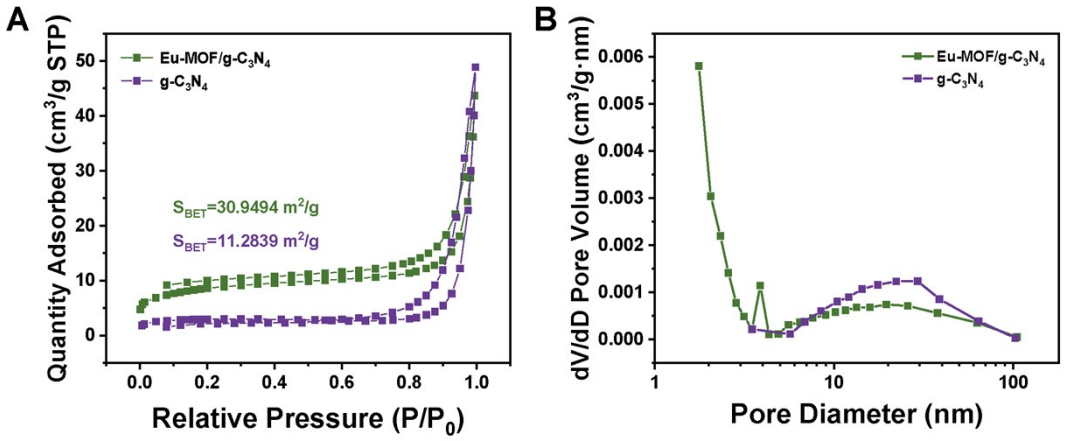

Fig. S3. (A) N_2 adsorption-desorption isotherms of g-C_3N_4 and Eu-MOF. (B) Pore size distribution curves of g-C_3N_4 and Eu-MOF.

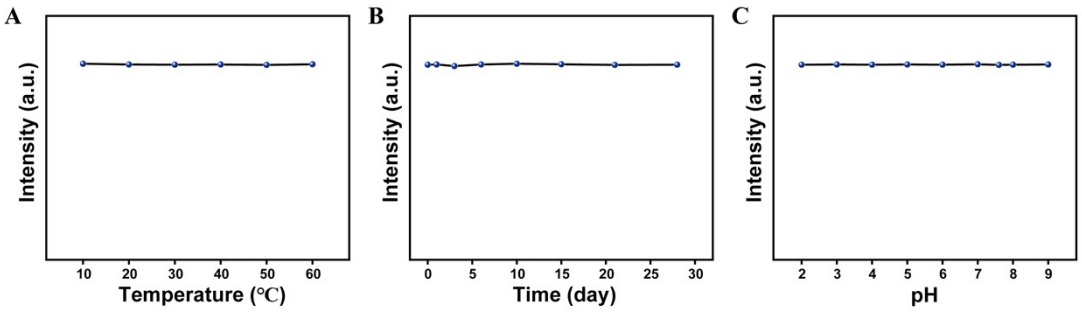

Fig. S4. Fluorescence stability of Eu-MOF/g-C_3N_4 at different (A) temperatures, (B) storage durations, (C) pH values.

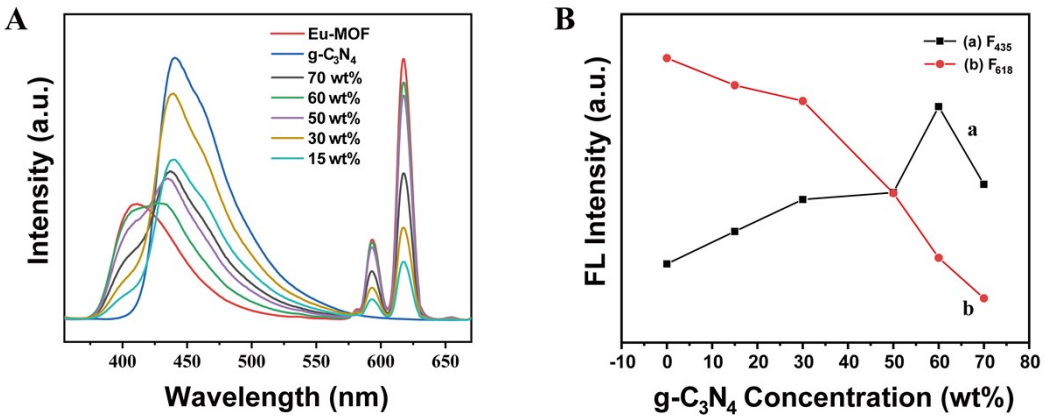

Fig. S5. (A) and (B) The amount of g-C_3N_4 added to the fluorescence emission intensity of Eu-MOF/g-C_3N_4.

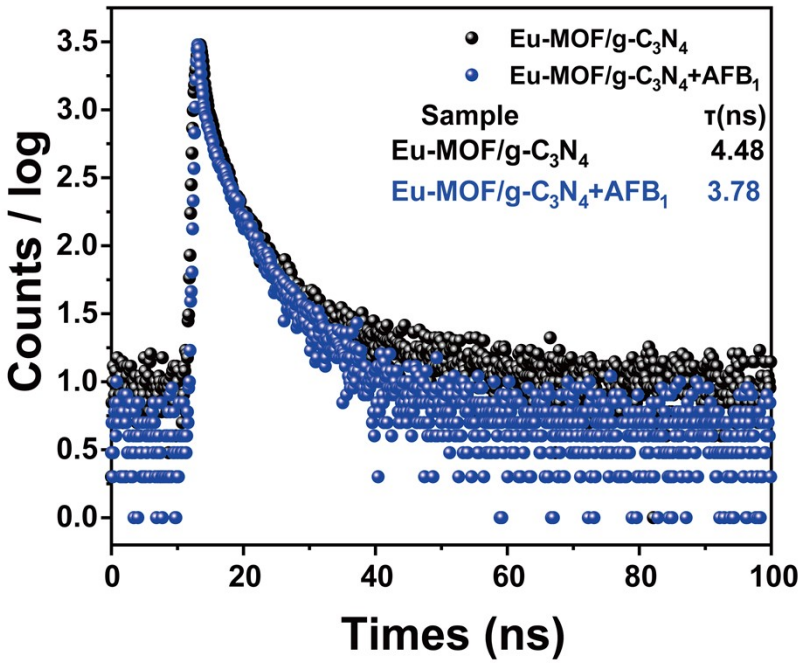

62

63 **Fig. S6.** FL lifetimes of Eu-MOF/g-C_3N_4 with and without the presence of AFB_1.

64

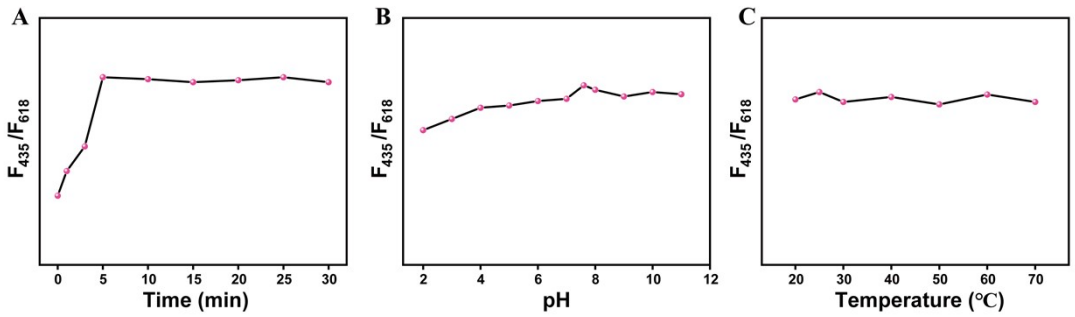

Fig. S7. Fluorescence response of Eu-MOF/g-C_3N_4 to AFB_1 for different (A) reaction times, (B) pH values, and (C) reaction temperatures of sensing system.

Fig. S8. Fluorescence for simultaneous detection and degradation.

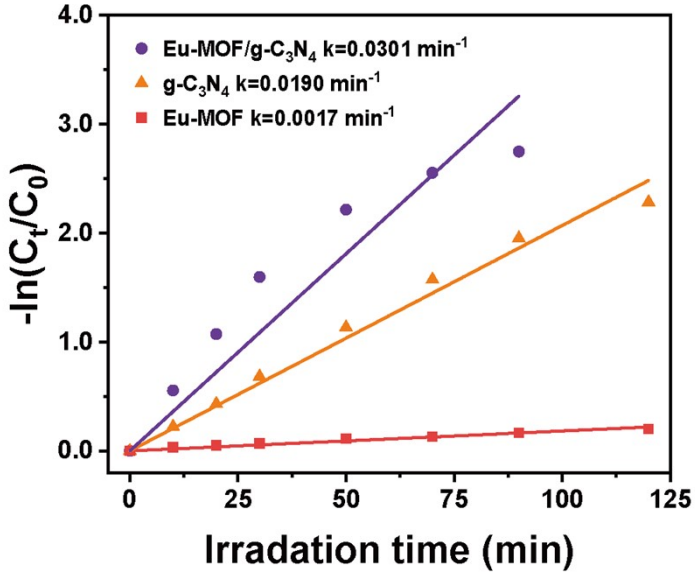

72

73 **Fig. S9.** Pseudo-first-order kinetic fitting curves of Eu-MOF/g-C_3N_4, g-C_3N_4 and Eu-

74 MOF.

75

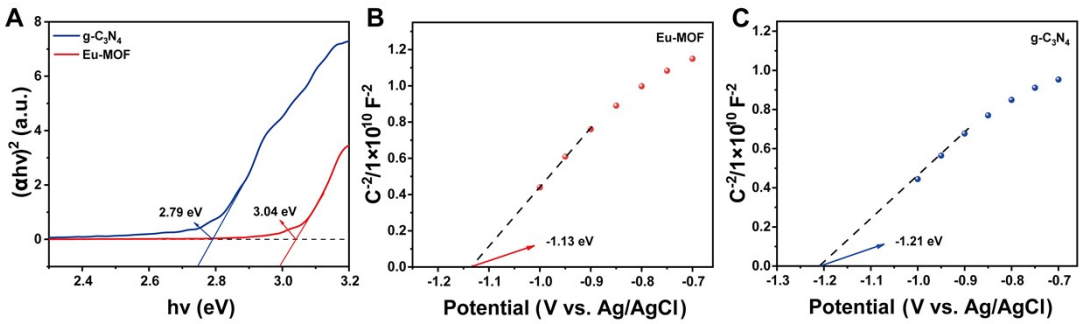

Fig. S10. (A) Band gap energies of Eu-MOF and g-C_3N_4. Mott-Schottky plots of Eu-MOF(B), and g-C_3N_4 (C).

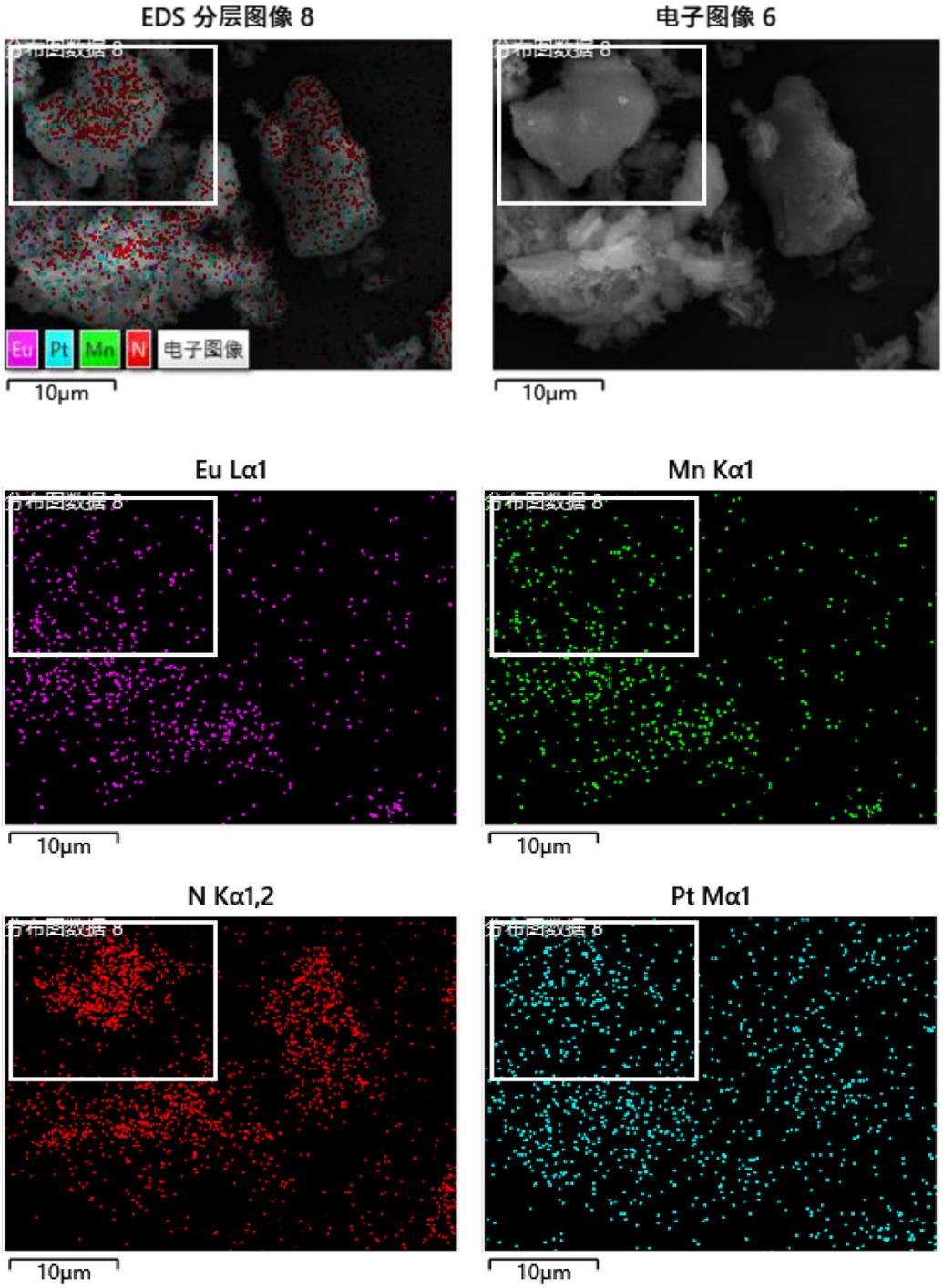

Fig. S11. SEM-EDS spectra of Eu-MOF/g-C_3N_4 after photodeposition experiment.

Note: The selected areas in the figure show that Pt overlaps more with the N element of carbon nitride, meaning that Pt is mainly deposited on carbon nitride, and electrons accumulate on g-C3N4. Mn overlaps more with Eu, indicating that Mn is deposited on Eu-MOF, which is a hole-rich site. According to the band data and the spatial distribution results of photodeposited Pt and Mn, this is a Z-scheme heterojunction.

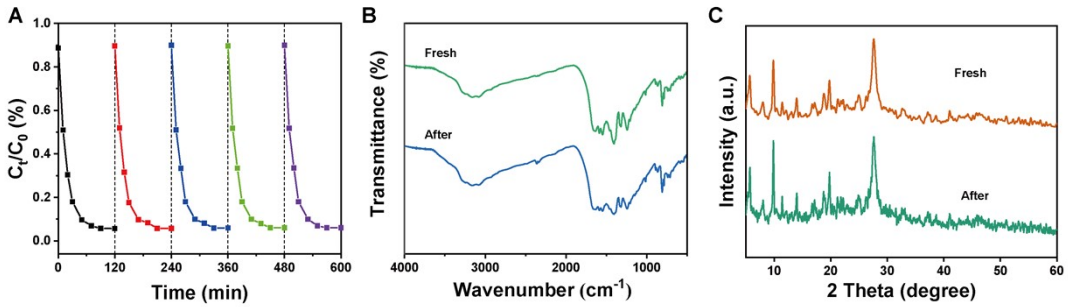

Fig. S12. (A) Degradation efficiency chart of Eu-MOF/g-C3N4 after five consecutive test cycles. (B) FT-IR and (C) XRD spectra before and after cyclic degradation experiments.

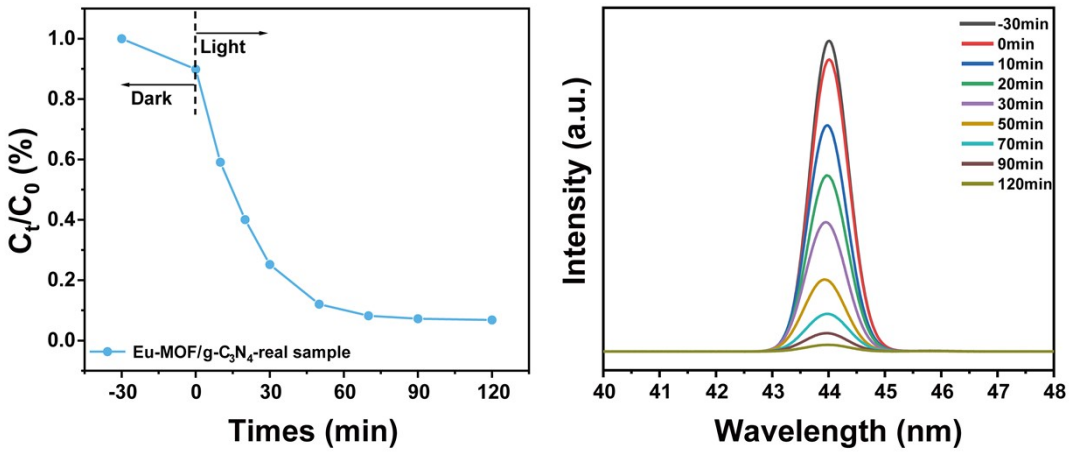

93

94 **Fig. S13.** (A) Photocatalytic degradation efficiency and (B)HPLC chromatograms of
95 AFB_1 degradation in peanut oil samples by Eu-MOF/g-C_3N_4 under visible light
96 irradiation with different durations.

97

Table S1. Comparison Table of MOF based AFB_1 Detection and Degradation Systems.

Materials	Function	Mechanism	LOD (ppb)	Degradation efficiency	Limitation	Ref
Al-MOF	Detection only	Single emission	11.67	N/A	High detection limit; single transmission	[1]
LMOFs	Detection only	Single emission	19.97	N/A	Lower sensitivity	[2]
Zr-MOF	Detection only	Single emission	0.5	N/A	Complex adapter modification; Non visual detection	[3]
GO/$Cu_3(BTC)_2$ /Fe_3O_4	Degradation only	Photocatalysis	N/A	96.8%	Stability to be verified; Degradation conditions not optimized	[4]
MAgPW	Degradation only	Photocatalysis	N/A	85%	Low degradation rate	[5]
g-C_3N_4/ CQDs/MoS_2	Degradation only	adsorption-photocatalysis	N/A	96.8%	Membrane preparation is complex; MoS_2 may oxidize	[6]
Cu-NH_2-BDC/Ag_2S	Detection +Degradation	Photoelectrochemical +Photocatalysis	0.29	98%	Extremely complex synthesis; No visual detection;	[7]
Eu-MOF/g-C_3N_4	Detection +Degradation	Ratiometric fluorescence +Photocatalysis	11.48	94.33%	This work	This work

Table S2. Detection of AFB_1 in real samples (n = 3).

Sample	Spiked (μM)	Found (μM)	Recovery (%)	RSD (%, n = 3)
Peanut oil	0.1	0.0984	98.4	1.21
	0.5	0.487	97.4	1.32
	1.0	1.012	101.2	1.61
	2.5	2.489	99.56	0.95
	5.0	5.011	100.22	0.33

The above results are the average of three repeated experiments.

References

1. F. X. Wang, Z. P. Li, H. P. Jia, R. H. Lu, S. B. Zhang, C. P. Pan and Z. Q. Zhang, *Food Chemistry*, 2022, **383**.
2. Z. S. Li, X. H. Xu, Y. C. Fu, Y. N. Guo, Q. Zhang, Q. Y. Zhang, H. Yang and Y. B. Li, *Rsc Adv*, 2019, **9**, 620-625.
3. X. B. Li, F. X. Meng, Z. D. Li, R. Z. Li, Y. K. Zhang and M. W. Zhang, *Sensor Actuat B-Chem*, 2023, **394**.
4. M. S. Samuel, K. Mohanraj, N. Chandrasekar, R. Balaji and E. Selvarajan, *Chemosphere*, 2022, **291**.
5. P. Meng, J. Li, P. Wang, G. Yang, W. Liu, S. Liang, R. Yang and C. Sun, *Chem Eng J*, 2024, **483**.
6. R. X. Song, L. T. Yao, C. P. Sun, D. C. Yu, H. Lin, G. S. Li, Z. C. Lian, S. L. Zhuang and D. W. Zhang, *Toxins*, 2023, **15**.
7. X. Du, Z.-Y. Feng, B. Jin and L.-Y. Meng, *Surfaces and Interfaces*, 2025, **73**.